

Colloid lithography-induced polydimethylsiloxane microstructures and their application to cell patterning

Dong Kee Yi^{1,4}, Min Jun Kim^{2,3}, Linda Turner³, Kenneth S. Breuer² & Dong-Yu Kim^{4,*}

¹*Institute of Bioengineering and Nanotechnology, Singapore 138669, Singapore*

²*Division of Engineering, Brown University, Providence RI 02192, USA*

³*Rowland Institute at Harvard, Cambridge MA 02142, USA*

⁴*Center for Frontier Materials, Gwangju Institute of Science and Technology, Gwang-Ju 500-712, Republic of Korea*

**Author for correspondence (Fax: +82-062-970-2330; E-mail: kimdy@kjist.ac.kr)*

Received 26 August 2005; Revisions requested 23 September 2005; Revisions received 10 November 2005; Accepted 11 November 2005

Key words: cell patterning, colloidal lithography, honeycomb structures, micro-rings, *Serratia marcescens*

Abstract

Colloidal lithography was used to make a novel array (2-D) of micro-rings, dots, and interconnected-honeycomb structures. These geometries are controlled using the curing temperature-dependent rheological properties of the siloxane elastomer precursor. *Serratia marcescens* was patterned on the interconnected honeycomb microstructure demonstrating a potential application for microbioanalytical devices, microfluidics, and bio-micro-electromechanical systems.

Introduction

Soft lithography (Xia & Whitesides 1998) is a powerful micro-fabrication technique for creating convenient, low-cost, and biologically compatible devices. Such devices can be used in conjunction with other technologies such as micro-electromechanical systems (MEMS) and microfluidics to fabricate microbioanalytical devices (Ziegler & Fresenius 2000, Zlauddin & Sabatini 2001). However, in soft lithography, template formation usually requires a polydimethylsiloxane mold fabricated via a photolithographic mask and an energy source: the template is not independent from the photolithographic method. Recently, self-assembled colloidal structures were introduced as a template for fabricating three-dimensional inverse opals (Gates *et al.* 1999, Wang & Caruso 2001, Jiang *et al.* 2001), and 2-D inorganic (Hulteen *et al.* 1999, Burmeister *et al.* 1997) or protein nanostructures (Carno *et al.* 2002). In this communi-

cation, we demonstrate that the colloidal monolayer works as a novel polydimethylsiloxane patterning mask, circumventing the use of the photolithographic method, and that the resulting polydimethylsiloxane structures can be used to pattern a bacterium, such as *Serratia marcescens*, into geometric arrays.

There are several reasons for wishing to pattern cells: patterned cells can be used in biosensor, neuronal network systems, tissue engineering, and miniaturized drug screening assay. Our technique uses an easily controllable process and a simplified patterning strategy. It does not use a biochemical cell coordinator, such as ethylene glycol as non-cell fouling agent (Lopez *et al.* 1993, Ghosh *et al.* 1999), or mediating proteins to attach cells (Mrksich *et al.* 1997). In those approaches, a polydimethylsiloxane stamp regulates the patterning of the biochemical cell coordinator which coordinates the cells. Here, the polydimethylsiloxane architecture patterns the bacterium, *Serratia marcescens*.

Materials and methods

Serratia marcescens was grown on swarm plates composed of LB-broth (Bacto-tryptone 10 g/l, yeast extract 5 g/l, and NaCl 5 g/l) containing 0.6% Difco Bacto-agar at 30 °C according to the methods of Darnton *et al.* (2004). Bacteria were washed free from the swarm plate surface using motility buffer (0.01 M KPO_4 buffer pH 7, 0.067 M NaCl, 10^{-4} M EDTA, and 0.002% Tween 20) then fluorescently labeled with Cy 3 (PA23001, Amersham Pharmacia) according to Turner *et al.* (2000). The labeled bacteria were added back to a swarm plate and a bacterial carpet prepared by blotting according to Darnton *et al.* (2004). The resulting bacteria coated surfaces were imaged in a Nikon inverted microscope equipped for fluorescence.

The siloxane elastomer used for making patterns was Dow Corning brand Silicone Encapsulants (Form No. 10-898C-01). Our approach to creating the patterns starts with a 2-D polystyrene colloid (diam. = 4 μm , Duke Scientific, Palo Alto, CA) monolayer with hexagonal order, formed by convective crystallization (Velev *et al.* 1992) on a glass microslide [cleaned in a hot mixture of $\text{H}_2\text{SO}_4/\text{H}_2\text{O}_2$ (7/3 v/v) for 4 h, and washed with deionized water]. During the colloidal crystallization, the colloids adhere on the microslide strongly due to the capillary forces. The siloxane pre-polymer (Sylgard 184, Dow Corning) was degassed in vacuo and coated over the 2-D colloidal monolayer at either 105 °C or 25 °C, and cross-linked for 1 h at 105 °C and for 50 h at 25 °C (see Figure 1). The prepolymer was not pressurized during the coating process. Subsequently, the polydimethylsiloxane elastomer was peeled off using sticky tape and the colloids etched by dipping into a toluene bath for 48 h. Peeling created two polydimethylsiloxane templates, a thicker upper one and a thinner lower one (see middle diagram of Figure 1). We concentrated our efforts on the lower one, which after toluene etching showed two kinds of patterns: a combined structure of rings and dots (Figures 1a, 2a) and a 2-D honeycomb (Figures 1b, 2b, c). We imaged the templates by optical microscopy (Olympus MX 40) and atomic force microscopy, Digital Instrument Nanoscope III.

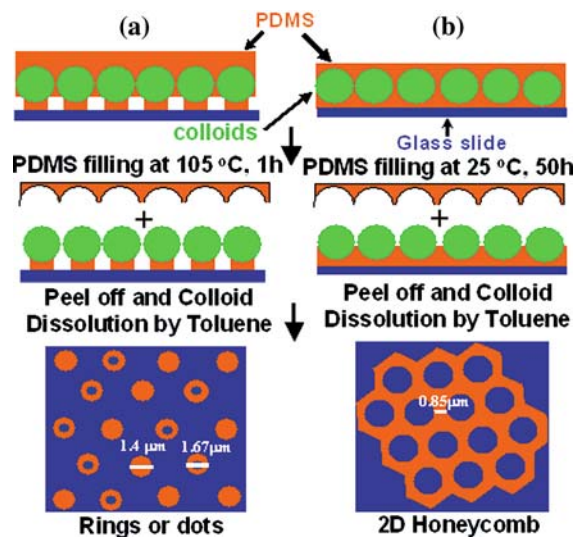


Fig. 1. Siloxane elastomer was infiltrated into the 2-D polystyrene monolayer under (a) 105 °C, curing 1 h, or (b) room temperature, curing 50 h. The lower peel-off part was etched by toluene for 48 h, and subsequently rings (diam. = $\sim 1.67 \mu\text{m}$), dots (diam. = $\sim 1.4 \mu\text{m}$) or 2-D honeycomb (bridge width $\sim 0.85 \mu\text{m}$) were achieved.

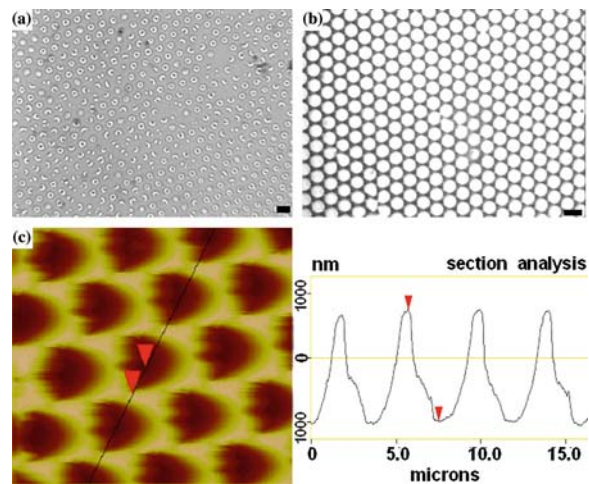


Fig. 2. (a) Optical micrographs of rings and dots fabricated when the silicon elastomer was cured at 105 °C for 1 h, (b) however after room temperature curing, 2-D interconnected patterns were observed (scale bars, 5 μm). (c) Atomic force microscopy depth profile of 2-D honeycomb structure. The skewing structure of honeycomb is clear.

Results and discussion

The two different patterns originated due to the polydimethylsiloxane curing temperature. When the curing temperature is high (105 °C), the cross-

linking process is accelerated, and infiltration into the 2-D colloidal monolayer is incomplete, producing discrete geometries (dots or rings). Atomic force microscopy analysis showed that the average ring diameter is $1.67 \pm 0.12 \mu\text{m}$ and the height is $58 \pm 6 \text{ nm}$ and the average dot diameter is $1.4 \pm 0.06 \mu\text{m}$ and the height is $86 \pm 13 \text{ nm}$ (see Figure 3). This effect is due to both the high viscosity of the siloxane elastomer caused by the fast curing effect (siloxane elastomer curing time is disproportional to the curing temperature) and the increase of colloidal packing density (colloid–colloid neck formation at high temperature) (Yi & Kim 2003a, b). When the temperature increased to $115 \text{ }^\circ\text{C}$ (curing time 40 min), colloid–colloid neck formation became clearer and the masking effect becomes even stronger allowing only a small quantity of siloxane elastomer to penetrate the mask. In this case, polydimethylsiloxane was found in the vacant triangular area where the nearest three colloids meet and subsequently isolated dots form in a hexagonal pattern (see Figure 4a). However, when the curing temperature was low ($25 \text{ }^\circ\text{C}$), the siloxane infiltrated the colloidal structure thoroughly, resulting in an interconnected 2-D honeycomb polydimethylsiloxane pattern (Figures 1b, 2b, c). The walls of the honeycomb were skewed because of the circular shaped colloids.

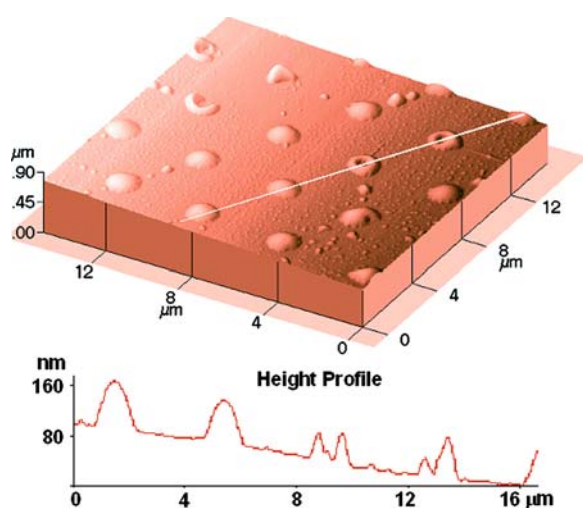


Fig. 3. Atomic force microscopy depth profile of ring and dot structures of polydimethylsiloxane. The average ring diameter is $1.67 \pm 0.12 \mu\text{m}$ and the height is $58 \pm 6 \text{ nm}$ and the average dot diameter is $1.4 \pm 0.06 \mu\text{m}$ and the height is $86 \pm 13 \text{ nm}$.

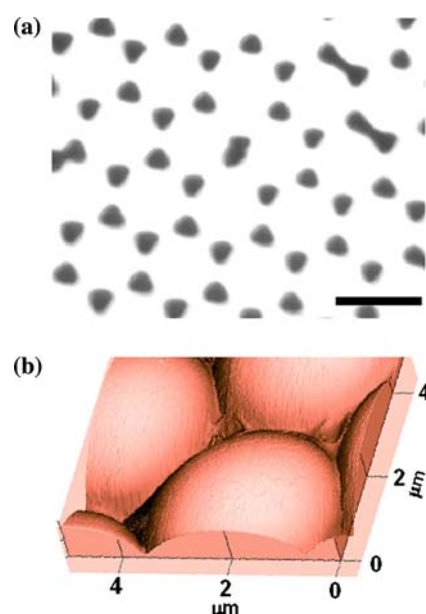


Fig. 4. (a) Optical micrograph of hexagonal polydimethylsiloxane patterns observed when the silicon elastomer was infiltrated and cured at $115 \text{ }^\circ\text{C}$. Scale bar, $5 \mu\text{m}$. (b) Atomic force microscopy image shows the concave torn traces in the tripod area after peeling off the room temperature cured polydimethylsiloxane.

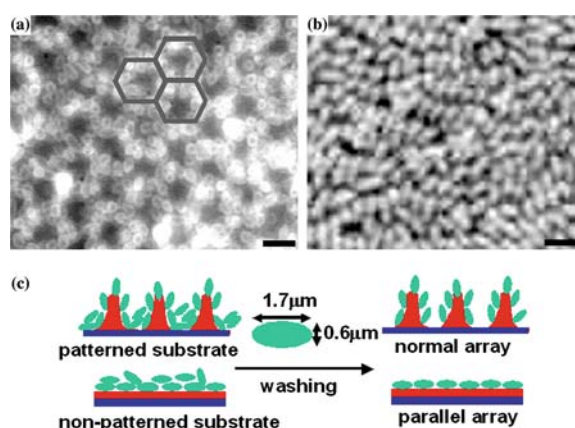


Fig. 5. (a) Optical micrograph of hexagonal patterned fluorescent bacterial cells and (b) bacterial cells on the non-patterned flat polydimethylsiloxane (bacteria are bright against a dark background). Hexagonal grids in (a) represent the patterned polydimethylsiloxane templates. Scale bar $3 \mu\text{m}$. (c) Schematic views of bacteria adsorption on the polydimethylsiloxane substrate; green ellipsoids, blue layer, and red layer represent bacteria, glass slide, polydimethylsiloxane, respectively. Bacteria on the patterned substrates show standing array predominant; however, ones on the non-patterned substrates showed lying array, predominant.

To monitor infiltration, we studied the lower part peel-off surface (Figure 1b mid) still containing colloids using atomic force microscopy. Concave peel-off traces were clearly visible in the tripod area (Figure 4b) and, furthermore, the atomic force microscopy depth profile showed that the resulting colloid-free 2-D honeycomb polydimethylsiloxane has much greater height, $1.85 \pm 0.14 \mu\text{m}$, compared to those of the dot or ring structure. From this evidence, we conclude that siloxane prepolymer was thoroughly infiltrated within the 2-D colloidal monolayer, thus fabricating 2-D interconnected bridges, width $0.85 \pm 0.12 \mu\text{m}$, at 25°C (Figure 2c).

The 2-D honeycomb polydimethylsiloxane pattern was further studied to check whether it is feasible as a substrate for patterning cells. For comparison we also examined bacterial adsorption on the non-patterned, flat polydimethylsiloxane. Figure 5(a) shows the hexagonal patterned bacteria along the 2-D honeycomb of polydimethylsiloxane. These bacteria are viable on the patterned substrate. Attachment to the substrate appeared to be regulated by hydrophobic (polydimethylsiloxane) and hydrophilic (glass) interactions. We speculate that the hydrophilic glass surface prohibits the formation of a protein layer that mediates cell adherence (Lopez *et al.* 1993, Mrksich *et al.* 1997, Ghosh *et al.* 1999). The bacteria were not adsorbed on the clean glass surface after rinsing.

The patterned bacteria were mostly standing on end, normal to the substrate (average number of bacteria $36.3 \pm 0.8/100 \mu\text{m}^2$). However, when bacteria were attached on the non-patterned polydimethylsiloxane, they were mostly lying flat with their long axis in contact with the surface. In this attachment mode alignment occurred over short distances ($10 \mu\text{m}$) with no long range correlation and the packing density was lower, $32.2 \pm 4.3/100 \mu\text{m}^2$ (Figure 5b). However, the patterned substrate is an array with empty glass holes, whereas the non-patterned substrate is continuous. Image analysis data, performed using a Quantimet 570 image analyzer (Cambridge Instrument), shows that the polydimethylsiloxane area proportion in the patterned substrate is only 34%. Since the bacterium is rod shaped ($\sim 0.62 \mu\text{m}$ wide by $\sim 1.7 \mu\text{m}$ long), the standing-mode array on the patterned

substrate resulted in a higher bacterial adsorption compared to the lying-mode on the non-patterned substrate. Figure 5(c) shows the proposed schematic diagrams for the adsorption of bacteria according to two different array modes. Additionally, the skewing structure (see atomic force microscopy image in Figure 2c) of the honeycomb wall can increase the area for the adsorption of bacteria. Therefore the actual polydimethylsiloxane area proportion could be larger than the measured 34% and help to increase the packing density. Although it is not clear to us why the bacterial arraying mode is different, we conclude that the patterned architecture successfully induced ordered cell patterning.

A recent study of the flagella of group of bacteria shows that substrate-fixed, living bacteria can be used as micro-mechanical units (Darnton *et al.* 2004, Kim & Breuer 2005). In terms of power efficiency, a highly concentrated bacterial pattern could be desirable.

Conclusions

Cross-linking of polydimethylsiloxane prepolymer has been achieved under controlled rheological conditions to create 2-D micro rings, dots, and 2-D interconnected honeycomb structures using 2-D colloidal templates. 2-D *Serratia marcescens* patterning was achieved along the resulting 2-D interconnected honeycomb structures. Remarkably, the 2-D interconnected honeycomb structures have higher induced packing density of *Serratia marcescens* compared to the case of using non-patterned flat polydimethylsiloxane substrate. The density difference could be due to the distinguished array modes of bacteria for both polydimethylsiloxane patterns, 2-D honeycomb and flat, respectively. We believe that our patterned bacteria structure has potential in microbioanalytical devices, microfluidics, and bio-micro-electromechanical systems.

Acknowledgements

This work has been supported by the DARPA BioMolecular Motors Program (DARPA BAA 01-47).

References

- Burmeister F, Schafle C, Matthes T, Bohmisch M, Boneberg J, Leiderer P (1997) Colloid monolayers as versatile lithographic masks. *Langmuir* **13**: 2983–2987.
- Carno JC, Amro NA, Wadu-Mesthrige K, Liu GY (2002) Production of periodic arrays of protein nanostructures using particle lithography. *Langmuir* **18**: 8186–8192.
- Darnton N, Turner L, Breuer K, Berg HC (2004) Moving fluid with bacterial carpets. *Biophysic. J.* **86**: 1863–1870.
- Gates B, Yin Y, Xia Y (1999) Fabrication and characterization of porous membranes with highly ordered three-dimensional periodic structures. *Chem. Mater.* **11**: 2827–2836.
- Ghosh P, Amirpour ML, Lackowski WM, Pishko MV, Crooks RM (1999) A simple soft lithographic approach for preparing patterned, micron-scale corrals for controlling cell growth. *Angew. Chem. Int. Ed.* **38**: 1592–1595.
- Hulteen JC, Treichel DA, Smith MT, Duval ML, Jensen TR, Dwyne RPV (1999) Nanosphere lithography: size-tunable silver nanoparticle and surface cluster arrays. *J. Phys. Chem. B.* **103**: 3854–3863.
- Jiang B, Bertone JF, Colvin VL (2001) A lost-wax approach to monodisperse colloids and their crystals. *Science* **291**: 453–457.
- Kim MJ, Breuer KS (2005) Characteristics of bacterial pumps in microfluidic systems. In: *2005 NSTI-Nanotechnology Conference and Trade Show*, May 8–14, Anaheim, Vol. 1, pp. 712–715.
- Lopez GP, Albers MW, Schreiber SL, Carroll R, Peralta E, Whitesides GM (1993) Convenient methods for patterning the adhesion of mammalian cells to surfaces using self-assembled monolayers of alkanethiolates on gold. *J. Am. Chem. Soc.* **115**: 5877–5878.
- Mrksich M, Dike LE, Tien J, Ingber DE (1997) Using microcontact printing to pattern the attachment of mammalian cells to self-assembled monolayers of alkanethiolates on transparent films of gold and silver. *Exp. Cell. Res.* **235**: 305–313.
- Turner L, Ryu WS, Berg HC (2000) Real-time imaging of fluorescent flagellar filaments. *J. Bacteriol.* **182**: 2793–2801.
- Velev OD, Kralchevsky PA, Ivanov IB, Yoshimura H, Nagayama K (1992) Mechanism of formation of two-dimensional crystals from latex particles on substrates. *Langmuir* **8**: 3183–3190.
- Wang D, Caruso F (2001) Fabrication of polyaniline inverse opals by templating ordered colloidal assemblies. *Adv. Mater.* **13**: 350–354.
- Xia YN, Whitesides GM (1998) Soft lithography. *Annu. Rev. Mater. Sci.* **28**: 153–184.
- Yi DK, Kim DY (2003) Novel approach to the fabrication of macroporous polymers and their use as a template for crystalline titania nano rings. *Nanoletters* **3**: 207–211.
- Yi DK, Kim DY (2003) Polymer nanosphere lithography: fabrication of an ordered trigonal polymeric nanostructure. *Chem. Commun.* **8**: 982–938.
- Yicong W, Ping W, Xuesong Y, Gaoyan Z, Huiqi H, Weimin Y, Xiaoxiang Z, Jinghong H, Dafu C (2001) Drug evaluations using a novel microphysiometer based on cell-based biosensors. *Sens. Actuators B.* **80**: 215–221.
- Ziegler C, Fresenius J (2000) Cell-based biosensors. *Anal. Chem.* **366**: 552–559.
- Zlauddin J, Sabatini DM (2001) Microarrays of cell expressing defined cDNAs. *Nature* **411**: 107–110.